Site-Selective Photochemistry in an Alternating 2-Norbornyl−CO Copolymer: Importance of Stereoelectronic Effects

Malcolm D. E. Forbes,*,† Shiyamalie R. Ruberu,† Dana Nachtigallova,‡ Kenneth D. Jordan,*,‡ and James C. Barborak§

Contribution from Venable and Kenan Laboratories, Department of Chemistry, CB #3290, University of North Carolina at Chapel Hill, Chapel Hill, North Carolina 27599, Department of Chemistry, Chevron Science Center, University of Pittsburgh, Pittsburgh, Pennsylvania 15260, and Department of Chemistry, University of North Carolina at Greensboro, Greensboro, North Carolina 27412

Received September 6, 1994[⊗]

Abstract: The electronic structure of a highly stereoregular, alternating 2-norbornyl−CO copolymer has been investigated using *ab initio* calculations on model compounds, and the photochemical consequences of these calculations are discussed in regard to recent laser flash photolysis/time resolved electron paramagnetic resonance (TREPR) experiments on this polymer. The polymer is believed to be synthesized in the *exo-syn* geometry. While photolysis is expected to lead to *exo*-substituted 2-norbornyl radicals, only *endo*-substituted radicals could be detected in the TREPR experiment. Evidence is presented that the *endo* radicals arise from selective photochemistry at *anti* defect sites in the polymer chain. NMR results from a ^{13}CO-enriched sample show that enol formation can be responsible for the disruption of the *exo-syn* stereochemistry along the polymer backbone. The *ab initio* calculations support the expectation of different photochemical reaction rates of the defects compared to the *exo-syn* linkages, due to the smaller electronic coupling matrix elements for triplet energy transfer at *anti* defect sites than at *exo-syn* linkages.

Introduction

Photodegradable polymers have received considerable attention due to their use in applications such as photoresists and packaging materials. Establishing the mechanism of degradation and possible side reactions in these polymers is a subject of intense interest in our laboratory.[1] We have recently reported a time-resolved electron paramagnetic resonance (TREPR) study of the solution photodegradation of two alternating alkyl−CO copolymers[1a] and identified the radical fragments produced in the primary photochemical events of their photodegradation. As shown in Scheme 1, in that work we found that while norbornyl−CO polymer **1** is believed to be synthesized with *exo-syn* stereoregularity (all −CO groups point toward the methylene group at C7), the dominant radical observed during the primary events of its photodegradation is in fact an *endo*-substituted 2-norbornyl radical. It was noted that such a radical can only be produced if the 2-norbornyl−CO copolymer is not completely stereoregular. In this paper we examine this interesting result in more detail, seeking to understand the origin of the loss of stereoregularity and the pronounced selectivity for the photochemical reaction to take place at the "defect" (*anti* or *endo*) sites rather than the "normal" (i.e. *exo-syn*) sites in the polymer. Below, we present new experimental results which provide strong evidence for the production of *endo*-substituted radicals which do not conflict with the characterization of the freshly synthesized polymer as predominantly *exo-syn*. Also, we report calculations showing that stereospecific electronic coupling exists in these macromolecules, leading to site-selective photochemistry.

Scheme 1

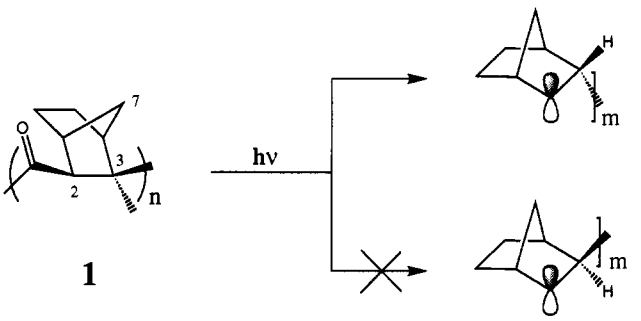

Results and Discussion

The previous EPR assignment is conclusively demonstrated by the spectral simulations shown in Figure 1, along with the TREPR data taken during the photolysis of **1** in benzene solution at room temperature. While both 3-*exo*- and 3-*endo*-substituted 2-norbornyl radicals have essentially the same splitting pattern, the *exo*-substituted radicals have a spectral width approximately 12 G narrower than the *endo*-substituted species, corresponding to the difference in the β-hyperfine coupling constants at position 3. This is due to the significant pyramidalization of the radical center at position 2, a characteristic of 2-norbornyl radicals which has been confirmed experimentally and theoretically in

* Authors to whom correspondence should be addressed.
† University of North Carolina at Chapel Hill.
‡ University of Pittsburgh.
§ University of North Carolina at Greensboro.
⊗ Abstract published in *Advance ACS Abstracts*, April 1, 1995.

(1) (a) Forbes, M. D. E.; Ruberu, S. R.; Dukes, K. E.; Barborak, J. C. *Macromolecules*, **1994**, *27*, 1020. (b) Forbes, M. D. E.; Myers, T. L.; Patton, J. T.; Wagener, K. B.; Maynard, H. D. *Polym. Prepr. (Am. Chem. Soc. Div. Polym. Chem.)* **1992**, *33(1)*, 883. (c) Patton, J. T.; Wagener, K. B.; Forbes, M. D. E.; Myers, T. L.; Maynard, H. D. *Polym. Prepr. (Am. Chem. Soc. Div. Polym. Chem.)* **1992**, *33(1)*, 1070. (d) Sheares, V. V.; Belu, A. M.; Dukes, K. E.; Linton, R. W.; Forbes, M. D. E.; DeSimone, J. M. *Polym. Prepr. (Am. Chem. Soc. Div. Polym. Mat. Sci. Eng.)* **1993**, *69(2)*, 247.

0002-7863/95/1517-3946$09.00/0

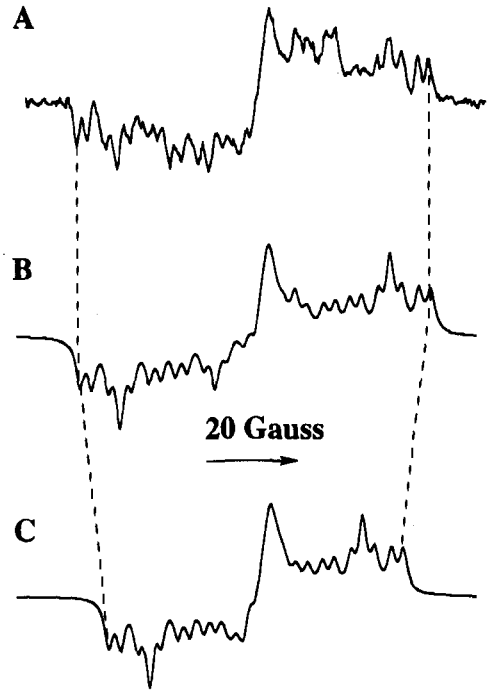

Figure 1. (a) TREPR spectrum obtained at a delay time of 1 μs after a solution of polymer **1** in benzene was laser flash photolyzed at 308 nm. (B) Simulation of the experimental data using literature parameters for a 3-*endo*-substituted 2-norbornyl radical. (C) What the simulation would look like using parameters for a 3-*exo*-substituted 2-norbornyl radical. The dashed lines show how much the spectral width changes when the hyperfine coupling constant of the proton at C3 is changed from 37.0 (*endo* substituent) to 25.0 G (*exo* substitutent). See ref 1a for more details regarding the assignment.

several laboratories.[2] Such a large difference in spectral width is well outside the experimental error of our data collection and simulation routines (<0.5 G). We note that in the center of the spectrum there are intensity differences unaccounted for in the simulation, and this may be due to the fact that there is a superposition of *endo*- and *exo*-substituted radical signals. However, the *endo* radicals, identified by their larger spectral width, are clearly the dominant signal carrier in the spectrum, and this is the focus of the present report. To our knowledge this is the first time that EPR spectroscopy of a radical fragment has been used to examine the stereoregularity of a polymer chain.

There has been a recent accumulation of experimental evidence to support the preference of an *exo-syn* geometry in the synthesis of **1**.[3] X-ray crystal structures (representative drawings are shown in Chart 1) of similar catalysis complexed to the norbornyl ring system after one and two cycles of the polymerization reaction have been reported by Brumbaugh et al.[4] (Chart 1, A) and Markies and co-workers[5] (Chart 1, B), respectively. These structures show that in both cases the *exo-syn* geometry is preferred during the synthesis. However, the results of force field (MM2) calculations of aldehyde-capped

Chart 1

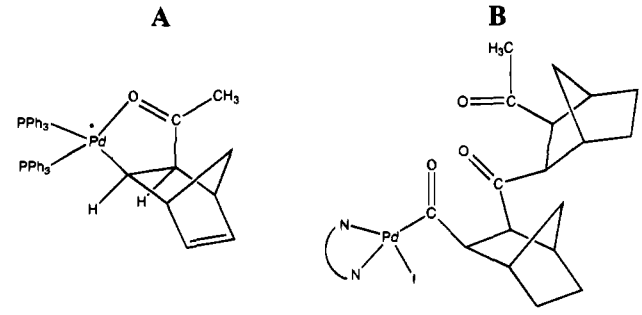

Table 1

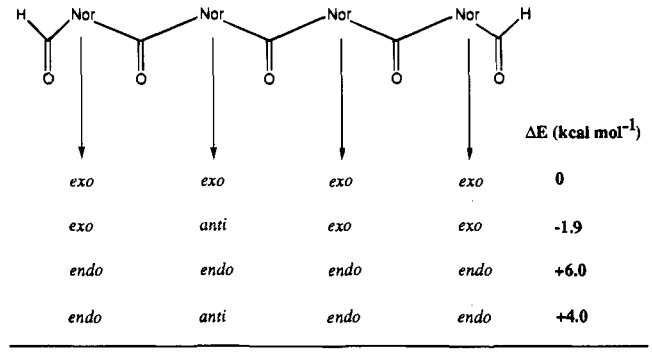

Chart 2

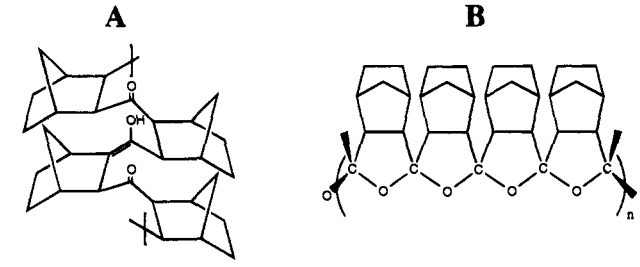

tetramers of the 2-norbornyl−CO system, listed in Table 1, show that an *exclusively exo-syn arrangement is not of lowest steric energy*.[6] As expected, the all *endo-syn* structure is of much higher steric energy than all other conformers that we examined. Therefore it is unlikely that the radicals we observe come from such a sequence. It is interesting to note that a lowering of the steric energy is also observed for the *endo-syn* geometry when an *anti* linkage is included in this structure.

Because the X-ray results and other mechanistic investigations[7] show that the *exo* geometry is preferred during the synthesis but may not lead to the thermodynamically most stable product, we have looked for mechanisms by which the original stereoregularity might be lost. Contact with strong bases could epimerize the ketones through the enolate, but this is unlikely as the freshly synthesized polymers are simply precipitated into methanol before they are characterized and the TREPR experiments are run immediately, *vide infra*. Epimerization through the enol form of the ketone, shown as structure A in Chart 2, is a more likely mechanism as it can be catalyzed simply by the presence of moisture in the sample after workup. Additionally, there is new evidence from two independent groups[8] that during the synthesis it is possible to have spiroketal formation, leading to the polymeric structure such as that shown as structure

(2) (a) Gloux, J.; Guglielmi, M.; Lemaire, H. *Mol. Phys.* **1970**, *19*, 833. (b) Marx, R.; Bonazzola, L. *Mol. Phys.* **1970**, *19*, 899. (c) Kawamura, T.; Koyama, T.; Yonezawa, T. *J. Am. Chem. Soc.* **1973**, *95*, 3220. (d) Kawamura, T.; Koyama, T.; Yonezawa, T. *J. Am. Chem. Soc.* **1970**, *92*, 7222. (e) Kawamura, T.; Suglyama, Y.; Yonezawa, T. *Mol. Phys.* **1977**, *33*, 1499. (f) King, F. W. *Chem. Rev.* **1976**, *76*, 157, and references thereln.

(3) Brookhart, M. S.; Rix, F. C.; DeSimone, J. M.; Barborak, J. C. *J. Am. Chem. Soc.* **1992**, *114*, 5894.

(4) Brumbaugh, J. S.; Whittle, R. R.; Parvez, M.; Sen, A. *Organometallics* **1990**, *9*, 1735.

(5) Markies, B. A.; Verkerk, K. A. N.; Rietveld, M. H. P.; Boersma, J.; Kooljman, H.; Spek, A. L.; van Koten, G. *J. Chem. Soc., Chem. Commun.* **1993**, 1317.

(6) The calculations were not run as global searches, since all we wished to show is that there are conformers that are of lower energy than the *exo-syn* one. There may be many others.

(7) Ozawa, F.; Hayashi, T.; Kolde, H.; Yamamoto, A. *J. Chem. Soc., Chem. Commun.* **1991**, 1469.

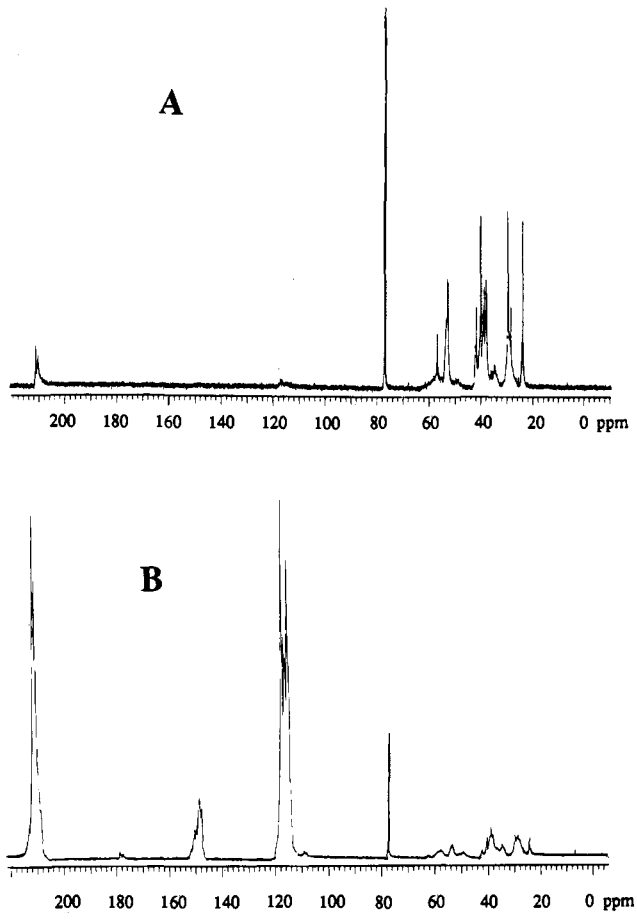

Figure 2. (A) ^{13}C NMR spectrum of a freshly synthesized sample of polymer **1** at natural abundance of ^{13}C. (B) ^{13}C NMR spectrum of a freshly synthesized sample of polymer **1**, where the carbonyl carbon has been enriched to 99% ^{13}C. See text for assignments.

B in Chart 2. However, no obvious pathway using this intermediate could be responsible for the scrambling of stereoregularity, since the α-H's in the norbornyl moiety are not involved in spiroketal formation. It should also be noted that there may simply be "mistakes" in the stereoregularity incorporated during the catalytic cycle. The one or two turnovers which led to the structures shown in Chart 1 are not statistically sufficient to conclude that the polymer is *perfectly* stereoregular. For further insight into the origins of the defect sites we turn to our NMR results on this polymer.

Figure 2 shows ^{13}C NMR spectra of freshly synthesized samples of polymer **1**. In Figure 2A, the CO carbon is at natural abundance, while in Figure 2B, this position has been enriched to 99% ^{13}C. It is clear by inspection of the carbonyl region at 210 ppm that neither polymer is perfectly stereoregular. For both samples there are two major peaks in this region. After enrichment, there are other major changes in the ^{13}C spectra. Several new peaks appear at chemical shifts of 115−120 and 146−152 ppm. The ^{1}H NMR spectra of these polymers do not change appreciably (there is some minor broadening in the ^{1}H spectrum of the enriched polymer due to long-range $^{13}C-H$ couplings). An important point is that there are no new transitions observed in the ^{1}H NMR spectrum of the enriched polymer, and we note also that no ^{1}H signals disappear upon ^{13}C enrichment. This leads us to conclude that the new transitions in the NMR of the ^{13}C-enriched polymer are due to carbon atoms that (1) originated from the enrichment site, i.e. the carbon atom in the −CO group, and (2) have no hydrogen atoms bonded to them. We assign the new peaks at 115−120 ppm to the spiroketal structure in structure B in Chart 2 (quaternary carbon) and the enol form of the ketone (C_α only) shown in structure A in Chart 2. The assignment for the quaternary carbon in the spiro compound is in agreement with those recently assigned to spiroketal carbon atoms in similar polymers by Wong et al.[8a] and by Batistini and Consiglio.[8b] The enol chemical shift is reported here only for the carbon next to the −OH group on the enol, since it is the only site that is enriched when the synthesis is carried out with ^{13}CO. There are no reports of ^{13}C NMR chemical shifts of norbornyl enols in the literature, but most alkyl-substituted enols appear at around 120 ppm. The signal at 146−152 ppm matches up well with ^{13}C chemical shifts for other sterically hindered enols reported by Nugiel and Rappoport,[9] but those were conjugated enols. In these polymers it is possible that this less intense signal arises from a conjugated "double enol", i.e., a butadiene-type structure that results from two adjacent enolized ketone sites. This assignment is at present only a speculation. Since our MM2 calculations provide evidence that the polymers favors *anti* linkages to some extent, the keto−enol tautomerization then provides a mechanism for such a transformation after the synthesis has already taken place. The reason we see such a strong signal for the enol is that the polymer is enriched (note that the enol signal is almost invisible in the natural abundance ^{13}C spectrum). Also, there may be a significant equilibrium population of the enol present in order to relieve steric crowding in the polymer. In ^{13}C NMR spectra of *tert*-butylstyrene−CO copolymers which were synthesized using the same catalyst and which were also studied in our earlier paper, no ^{13}C NMR signal from the enol was observed from an enriched sample. However, this polymer is much more flexible and less sterically hindered and therefore the enol may not have been present in a large enough concentration. There is an interesting qualitative difference in the signal intensity ratios of the spiroketal to carbonyl carbon NMR signals in Figure 2, spectra A and B. In the spectrum of the natural abundance polymer (Figure 2A), the carbonyl signal dominates, while in the spectrum of the enriched sample (Figure 2B), the spiroketal signal is comparable or even greater in intensity compared to the carbonyl peak. It is not likely that this difference could be due to any known remote isotope effect. An explanation might lie in other phenomena we do not yet understand, or more likely, in the fact that there were differences in the reaction conditions for the synthesis of the two samples (*vide infra*), since the spiroketal is the thermodynamic product.

The photochemical consequences of having an *exo-syn* polymer with *anti* "defect" sites are best illustrated by Figure 3. The carbonyl chromophores are aligned about 2.5 Å apart through space and are separated by only three σ bonds. Strong electronic coupling is therefore expected between the CO groups, and this coupling—both through-space (TS) and through-bond (TB)—may be substantially stronger for the *exo-syn* geometry than for the *anti* one. Strong coupling in a highly organized system such as that as that in Figure 3A may lead to rapid excitation transfer. An *anti* site such as that shown in Figure 3B can disrupt the excitation transfer if the coupling through this site is much weaker or if the excitation energy is lower at these sites causing them to act as traps. The low-lying singlet and triplet states of the polymers derive from the $n \rightarrow \pi^*$ excitations of the CO groups. Because the oscillator strengths of the singlet $n \rightarrow \pi^*$ excitations of the *exo*- and *endo*-norbornyls are near zero, singlet excitation transfer via the Förster mech-

(8) (a) Wong, P. K.; van Doorn, J. A.; Drent, E.; Sudmeijer, O.; Stil, H. A. *Ind. Eng. Chem. Res.* **1993**, *32*, 986. (b) Batistini, A.; Consiglio, G. *Organometallics* **1992**, *11*, 1766.

(9) Nugiel, D. A.; Rappoport, Z. *J. Am. Chem. Soc.* **1985**, *107*, 3669.

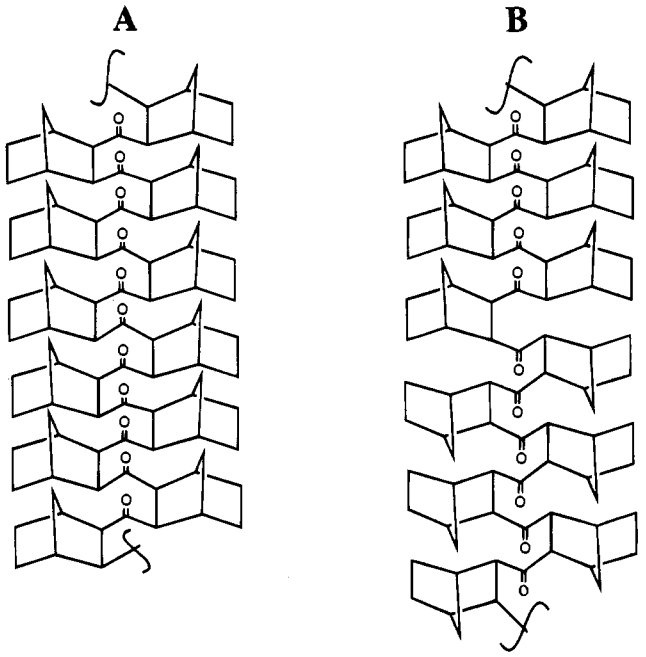

Figure 3. Polymer **1** drawn (A) exclusively in the *exo-syn* geometry and (B) with one *anti* linkage. Note that the polymer continues *exo-syn* after the lone *anti* "defect".

anism[10] is not expected to be important. On the other hand, both TB and TS coupling should be operative in both the singlet and triplet manifolds. The phase of the TREPR signals is emissive/absorptive which is the typical CIDEP pattern in normal organic solvents for radical pairs originating from triplet precursors.[11] This tells us that we are dealing with photochemical reactivity in the triplet state. Hence, we focus on the coupling in the triplet manifold, i.e., that which is responsible for Dexter energy transfer.[12]

Ab initio calculations[13] were carried out on the model systems shown in Chart 3 in order to determine the magnitude of the electronic coupling between the CO groups in the *exo-syn*, *endo-syn*, and *anti* forms of the polymer. To get a better understanding of contributions from TS interactions in the absence of those from TB interactions, formaldehyde (**2a**) and formaldehyde dimers in the *exo-syn* (**2b**), *endo-syn* (**2c**), and *anti* (**2d**) geometries were studied. Calculations on 2,3-norbornanedial in the *exo-syn* (**3a**), *endo-syn* (**3b**), and *anti* (**3c**) geometries gave couplings due to a sum of TS and TB effects. The splitting energy between the two lowest n $\rightarrow \pi^*$ states provides a measure of the electronic coupling in the triplet manifold. The excitation energies were calculated by means of the configuration interaction singles (CIS) method using the 3-21G basis set[14] and Hartree–Fock (HF)/STO-3G[15] optimized geometries. To test the suitability of the CIS method for calculating the splittings, we also carried out complete active space self-consistent field (CASSCF) and multi-reference MP2 (CASPT2)[16] calculations

Chart 3

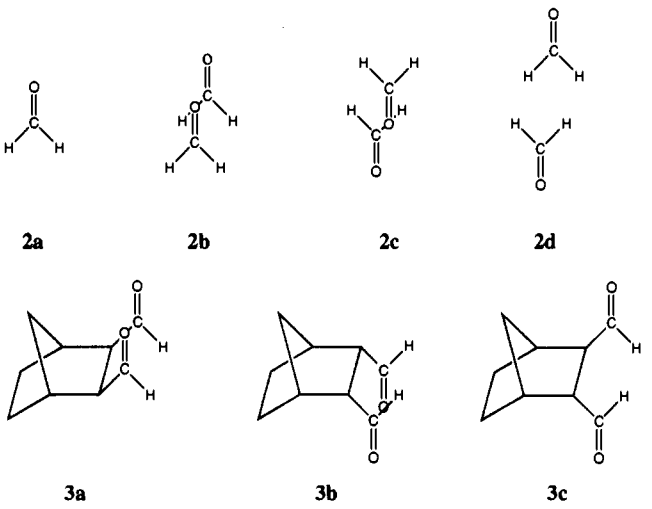

on the triplet states.[17] The latter procedure accounts for the dynamical electron correlation effects lacking in the CIS calculations. The CASSCF and CASPT2 calculations gave nearly the same splittings as obtained from the CIS calculations, and only the CIS results are considered in the remainder of the paper.

In order to interpret the results of the calculations, we find it useful to consider also the interactions between the lone pair (n) and the π^* orbitals. For this purpose we define the symmetry-adapted semilocalized orbitals:

$$n_+' = 1/\sqrt{2}(n_A + n_B) \qquad n_-' = 1/\sqrt{2}(n_A - n_B)$$

$$\pi_-{}^{*\prime} = 1/\sqrt{2}(\pi_A{}^* + \pi_B{}^*) \qquad \pi_+{}^{*\prime} = 1/\sqrt{2}(\pi_A{}^* - \pi_B{}^*)$$

where the n_A, $\pi_A{}^*$, n_B, and $\pi_B{}^*$ orbitals are localized on one or the other CO group, and the "+" and "−" combinations of the symmetry-adapted orbitals refer to the behavior under reflection in the symmetry plane (in the *exo-syn* and *endo-syn* compounds). Note that $\pi_-{}^{*\prime}$ and $\pi_+{}^{*\prime}$ refer respectively to the antibonding and bonding combinations of the $\pi_A{}^*$ and $\pi_B{}^*$ orbitals. The canonical n and π^* orbitals are then formed by mixing the n′ and $\pi^{*\prime}$ semilocalized orbitals with the other orbitals of the system of interest. Two low-lying covalent states and two higher-lying ionic states result from the mixing between the various n $\rightarrow \pi^*$ excitations. (In the *exo-syn* and *endo-syn* molecules the $n_+ \rightarrow \pi_+{}^*$ and $n_- \rightarrow \pi_-{}^*$ configurations mix as do the $n_+ \rightarrow \pi_-{}^*$ and $n_- \rightarrow \pi_+{}^*$ configurations. In the *anti* molecule, all four configurations mix together.) The electronic coupling in the triplet manifold is provided by the splitting between the two covalent triplet states. The n_+, n_- and $\pi_+{}^*$, $\pi_-{}^*$ splittings provide measures of the electronic coupling in the n and π manifolds, respectively. (Of course, strictly speaking, the "+" and "−" labels are not valid for the *anti* compound due to the lack of symmetry.)[18] The orbital splittings

(10) Förster, Th. *Discuss. Faraday Soc.* **1959**, *27*, 7.

(11) (a) *Spin Polarization and Magnetic Effects in Radical Reactions*; Molin, Yu. N., Ed.: Elsevier: New York, 1984. (b) McLauchlan, K. A. In *Advanced EPR: Applications in Biology and Biochemistry*; Hoff, A. J., Ed.; Elsevier: New York, 1990; pp 354–369. (c) Trifunac, A. D.; Lawler, R. G.; Bartels, D. M.; Thurnauer, M. C. *Prog. React. Kinet.* **1988**, *14*, 43.

(12) Dexter, D. L. *J. Chem. Phys.* **1953**, *21*, 836.

(13) Frisch, M. J.; Trucks, G. W.; Head-Gordon, M.; Gill, P. M. W.; Wong, M. W.; Foresman, J. B.; Johnson, B. G.; Schlegel, H. B.; Robb, M. A.; Replogle, E. S.; Gomperts, R.; Andres, J. L.; Raghavachari, K.; Binkley, J. S.; Gonzalez, C.; Martin, R. L.; Fox, D. J.; Defrees, D. J.; Baker, J.; Stewart, J. J. P.; Pople, J. A. *GAUSSIAN92*; Gaussian, Inc.: Pittsburgh, PA, 1991.

(14) Binkley, J. S.; Hehre, W. J.; Pople, J. A. *J. Am. Chem. Soc.* **1980**, *102*, 939.

(15) Hehre, W. J.; Stewart, R. F.; Pople, J. A. *J. Chem. Phys.* **1969**, *51*, 2657.

(16) Serrano-Andrés, L.; Merchán, M.; Fülscher, M. P.; Roos, B. O. *Chem. Phys. Lett.* **1993**, *62*, 400 and references therein.

(17) The CASSCF and CASPT2 calculations were carried out with the MOLCAS-3 program: Andersson, K.; Blomberg, M. R. A.; Fülscher, M. P.; Karlström, G.; Kello, V.; Lindh, R.; Malmqvist, P.-Å.; Noga, J.; Olsen, J.; Roos, B. O.; Sadlej, A. J.; Siegbahn, P. E. M.; Urban, M.; Widmark, P. O., University of Lund, Sweden.

(18) Also, in asymmetrical compounds such as **3c**, the electronic coupling should actually be determined by generating an effective two-level model rather than simply taking the orbital or state splittings as is done here.

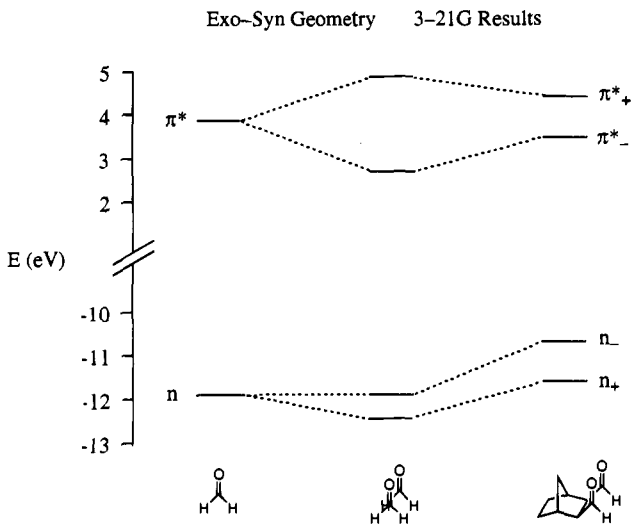

Figure 4. Correlation diagram showing HF/3-21G n and π^* orbital energies for formaldehyde (left), the formaldehyde dimer model **2b** (center), and 2,3-norbornanedial (**3a**) (right). The latter two model systems are in the *exo-syn* geometry.

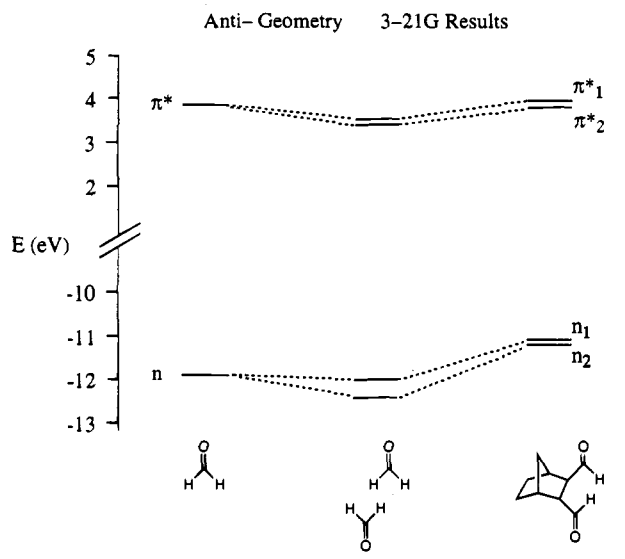

Figure 5. Correlation diagram showing HF/3-21G n and π^* orbital energies for formaldehyde (left), the formaldehyde dimer model **2d** (center), and 2,3-norbornanedial (**3c**) (right). The latter two model systems are in the *anti* geometry. Note that the "+" and "−" labelling system, which was used in the text and in Figure 4, is not used here because of the different local electronic environments for each CO group.

are obtained from HF/3-21G calculations on the ground states of the neutral molecules.

The orbital and triplet splittings obtained as outlined above are net splittings, containing contributions from both TS and TB interactions. To decompose the net interactions into TS and TB contributions, calculations were performed on the three formaldehyde dimer models (**2b**−**2d**), with the CO groups oriented as in the each of the norbornanedial molecules.[19] The splittings in the dimer models are taken as measures of the TS splittings in the "full" molecules (**3a**−**3c**).

A correlation diagram of the HF/3-21G energies of the n and π^* orbitals of formaldehyde, the formaldehyde dimer model of the *exo-syn* compound, and the *exo-syn* 2,3-norbornanedial is given in Figure 4. From this diagram it is seen that the TS interactions introduce sizable splittings in both the n and π^* manifolds and that the TB coupling increases the n_+, n_- and reduces the $\pi_+{}^*$, $\pi_-{}^*$ splittings (compared to their TS values). The net n_+, n_- and $\pi_+{}^*$, $\pi_-{}^*$ splittings are about 0.9 eV. The trends in the orbital splittings in the *endo-syn* compound are similar to those for the *exo-syn* compound.

A correlation diagram for the *anti* compound is shown in Figure 5. Both the TB and TS interactions are significantly reduced in the *anti* compound compared to the *exo-syn* and *endo-syn* compounds. The splittings in the *anti* compound have a contribution that arises from the fact that the two CO groups are in slightly different environments. If a correction is made for this environmental contribution, it is found that the net contribution of the TS and TB couplings to the orbital splittings in the *anti* compound is about eight times smaller than in the *exo-syn* compound.

We now consider the interactions in the triplet manifolds. A total of four triplet states can be formed upon $n \rightarrow \pi^*$ excitation in the 2,3-norbornanedials. We focus here on the splitting between the two lowest triplet states, since it is this splitting that provides a measure of the coupling responsible for excitation transfer. For the *exo-syn* and *endo-syn* species the CIS calculations give triplet splittings of 0.072 and 0.060 eV, respectively. These splittings indicate strong coupling and are consistent with rapid excitation transfer. The triplet splittings in the formaldehyde dimer models with the monomers arranged in the *exo-syn* and *endo-syn* orientations are 0.127 and 0.115 eV, respectively. Hence, for both isomers, the splitting between the lowest two triplet states is nearly two times smaller than in the corresponding formaldehyde dimer models. The smaller triplet splittings in the full molecules are due to the fact that TB and TS interactions act in opposite directions, as was found to be the case for the π^* orbitals.

The calculated splitting between the two lowest triplet states of the *anti* compound is 0.048 eV. However, the difference in the $n \rightarrow \pi^*$ excitation energies (0.052 eV) of the monoaldehydes (*endo-* and *exo*-2-norbornanal) is comparable in size to the splitting between the triplet states in the *anti* compound. This indicates that most of the splitting between the two lowest energy $n \rightarrow \pi^*$ triplet states of the *anti* compound is in fact due to the different environments of the two CO groups rather than to electronic coupling between these groups. Comparison of the $n \rightarrow \pi^*$ energies of the *exo*-norbornyl, the *endo*-norbornyl, and the *anti* compound leads to an estimate of 0.004 eV for the total (TB + TS) coupling in the *anti* compound. This is about 30 times smaller than the electronic coupling in the triplet manifolds of the *exo-syn* and *endo-syn* compounds. Analysis of the CI wavefunctions reveals that for the *anti* compound, the lowest triplet state is localized on the group with the *endo* orientation and that the excitation to this triplet state occurs about 0.05 eV lower in energy than that to the lowest triplet state of the *exo-syn* compound. These results suggest that an *endo* defect site in the *exo* form of the polymer should act so as to slow down excitation transfer along the polymer chain and may also act as a trapping site. This interpretation is consistent with the observed predominant bond cleavage at the *endo* sites.

Experimental Section

Synthesis of both samples of **1** (^{13}C-enriched and natural abundance) was conducted in a magnetically-driven medium-pressure stainless steel reactor from Parr Instrument Co. Norbornylene (Aldrich), serving as both reactant and solvent, was distilled immediately prior to use. ^{12}CO (CP grade, National Speciality Gases) was used directly from the cylinder without further purification. ^{13}CO (99% ^{13}C, 10% ^{18}O) was obtained from Cambridge Isotope Laboratories, Inc. The catalyst (0.1

(19) This approach to decomposing the interactions has been described in: (a) Paddon-Row, M. N.; Wong, S. S.; Jordan, K. D. *J. Chem. Soc., Perkin Trans.* **1990**, *2*, 425. (b) Falcetta, M. F.; Jordan, K. D.; McMurry, J. E.; Paddon-Row, M. N. *J. Am. Chem. Soc.* **1990**, *112*, 579.

mmol in both reactions) was the phenanthroline acetonitrile methyl palladium(II) tetrakis[bis(3,5-trifluoromethyl)phenyl]borate reported in ref 3. The reactions were conducted, insofar as possible, under identical conditions: CO pressure was initially 150 lbs; for ^{12}CO synthesis this pressure was maintained throughout the reaction, while in the ^{13}CO case the pressure was seen to drop as ^{13}CO was consumed. The reaction temperature was maintained at 70−75 °C for 168 h for the ^{12}CO polymer, and for 140 h in the ^{13}CO case. At the end of the reaction period the vessel was cooled to 45 °C and opened to the atmosphere. The grey reaction mixture was diluted with ~100 mL of methylene chloride and filtered through Celite filter aid. The CO−norbornylene copolymer was precipitated by slow addition of the filtered solution to ~600 mL of rapidly stirred methanol and collected by suction filtration. The white residue was washed several times with fresh methanol, then dried *in vacuo* overnight. The yield of copolymer from the ^{12}CO reaction was 10.0 g as an off-white powder, M_w = ~22 000 with a polydispersity of 1.90. The copolymer obtained in the ^{13}CO case was an off-white powder weighing 11.0 g with a M_w of ~29 000 and a polydispersity of 1.97. The IR spectrum of the ^{12}CO copolymer showed a carbonyl stretch at 1690 cm^{-1}, while the corresponding band appeared at 1652 cm^{-1} for the ^{13}CO copolymer.

Characterization of the polymers was performed using GPC, IR, and ^1H and ^{13}C NMR techniques. The gel permeation chromatograph was a Waters 1500-CV instrument equipped with Ultra Styragel columns of 100, 500, 10^3, 10^4, and 10^5 Å porosities. The FTIR measurements were carried out on a Biorad FTS-7 spectrometer, and ^1H and ^{13}C NMR measurements were carried out in $CDCl_3$ solution on a Varian XL-400 instrument using TMS as an internal standard.

Time-resolved EPR experiments were run on a JEOL, USA, Inc. JES-REIX spectrometer modified for direct detection with a fast preamplifier. Other components of the apparatus have been described previously.[1a] Samples of polymer in benzene solution (typical concentrations were 3 g per 100 mL) were flowed through a flat cell (0.5 mm) positioned in the center of a Varian TE_{103} optical transmission cavity. Nitrogen gas was bubbled through the samples for 10 min before and during each experiment.

Acknowledgment. This work was supported by the National Science Foundation through Grant No. CHE-9200917 (M.D.E.F.), Grant No. CHE-9121306 (K.D.J.), and the National Young Investigator Program (M.D.E.F., Grant No. CHE-9357108). The authors thank K. E. Dukes for experimental assistance, J. D. Ball for bringing ref 9 to our attention, and M. S. Brookhart and T. J. Meyer for helpful discussions.

JA942935J